

# Seismological criticality concept and percolation model of fracture

T. Chelidze,<sup>1,2</sup> Yu. Kolesnikov<sup>1</sup> and T. Matcharashvili<sup>1</sup>

<sup>1</sup>*Institute of Geophysics, Georgian Ac. Sci., 1, Alexidze str, Tbilisi, 0193, Georgia. E-mail: chelidze@ig.acnet.ge*

<sup>2</sup>*Tbilisi State University, 1, Melikishvili ave. Tbilisi, Georgia*

Accepted 2005 September 27. Received 2005 July 7; in original form 2004 March 19

## SUMMARY

In the present paper we consider an anisotropically correlated percolation model of fracture (PMF), namely, the geometry of fracture structures, the energy emission model and the evolution of scatter of emitted (effective) amplitudes at attaining the critical point (CP; percolation threshold). The sequences of effective amplitudes calculated from PMF are considered as proxies of seismic catalogues and are analysed by various linear and non-linear methods, developed in modern time-series analysis. It is shown that the drastic increase in the scatter of amplitudes is a good precursor of the impending CP even in the case of an individual percolation run. The Lempel-Ziv (LZ) complexity test reveals clear non-linear structure in the sequence of effective amplitudes; the value  $LZ = 0.750$  is significantly less than LZ for random process ( $LZ = 1$ ) and the Hurst exponent is in the range 0.8–0.85. Both these results point to the appearance of some order in the generation of effective emission events, due, probably, to the memory property of percolation processes. Various tests (curvature parameter, Shannon entropy) show that the acceleration of model seismicity close to the CP increases with the growth of anisotropic correlation (AC). The role of AC in the acceleration of energy emission, and Shannon entropy behaviour close to the CP, are analysed.

**Key words:** anisotropic correlation, criticality, effective amplitude, fracture, non-linear analysis, percolation.

## 1 INTRODUCTION

The two most popular paradigms for modelling seismic process are at present the theory of self-organized criticality (SOC) and the theory of critical point (CP). The former has been suggested by Bak *et al.* (Bak *et al.* 1988). T. Chelidze first suggested the percolation (CP) model of fracture and strong seismic events in 1978 (published: Chelidze 1980a,b, 1982). In the paper, under the title ‘Percolation and Fracture’ (1982) the percolation criticality model of fracture and seismic process as well as corresponding physical mechanism have been suggested; the first tests of critical (power-law) behaviour of precursors before failure of laboratory samples and some earthquakes have been done. The concentration of defects (microcracks) has been accepted as an order parameter. In 1982 the article (Allegre *et al.* 1982) was also published, where the similar idea was developed using renormalization group procedure.

The CP model considers the sequence of large events and following ‘stress shadows’ as evidence of corresponding stress build-up before, sudden stress drop during earthquake and residual stress relaxation during aftershock period. Thus, the seismic cycle is considered as approach to and retreat from the critical state of a fault network (intermittent criticality). After dynamical stress drop the internal friction of faults increases with time due to the healing action of high temperatures and confining pressures, giving a start to the new stress build-up process (Chelidze 1986).

The theory of self-organized criticality (SOC) was considered as a fundamentally different concept, because it envisions the Earth’s crust as a system that develops spontaneously to a permanent (statistically stationary) critical state, which is supported by the regular inflow of energy, particles, etc. The physical model of earthquake generation, supporting the SOC hypothesis, can be designed as a combination of a smooth drag term, due to the lithospheric plate motions, and an erratic component that is caused by the heterogeneity of lithosphere, fault roughness or just heterogeneous slip velocity. The heterogeneous component is responsible for such phenomena as fast creep, slow and genuine earthquakes.

In the pure SOC model large earthquakes are inherently unpredictable, because any small earthquake can evolve into a strong event: so a large event is just a small earthquake that did not stop. The CP theory, on the contrary, considers a large earthquake as a final result of some developing process (such as, say, clustering of microcracks towards the critical concentration, coinciding with the percolation threshold). This process is not statistically stationary; that is why the approaching final rupture can be predicted by monitoring the process of clustering of small faults, which affects almost all physical properties of the system (Chelidze 1982, 1986, 1987; Sornette 2000; Turcotte 2001).

In the beginning CP and SOC theories were considered as fully incompatible. Nevertheless, later on some hybrid models appeared (Huang *et al.* 1998; Newman & Turcotte 2002) that integrated these

two approaches. It has to be stressed that in hybrid models of SOC some allowance is always made for accumulation and relaxation of action: for example, some irregularities of the sand pile slope that cause transient deviations from the stationary state are introduced into the model. This leads to necessity of accumulation of several particles in the area of irregularity in order to launch an avalanche, which is similar to the stress build-up to the threshold value in the criticality approach. In the hybrid SOC + criticality model, suggested by Huang *et al.* (1998) the cell of the lattice becomes unstable only when it accumulates the threshold value of energy, which is then dissipated to the neighbouring sites. In this approach on the long timescale the network of faults generates seismic events that self-organize themselves into a stationary state with a power-law distribution of amplitudes. At the same time the process contains intermittent strong events with foreshocks and aftershocks; so the seismic process contains both stationary and non-stationary components. Similar conclusions follow from the hypothesis that the lithosphere is not permanently in a critical state, as is assumed in SOC, but in a subcritical state, which means that from time to time the system will experience large fluctuations (strong earthquakes) that are probabilistically predictable (Chelidze 2000). Main and Al-Kindy (Main & Al-Kindy 2002; Al-Kindy & Main 2003) examined entropy and energy in global and regional seismic catalogues and conclude that their results agree with a hypothesis that the earthquake machine works in a subcritical regime.

As the non-stationary component is artificially implemented into SOC by adding some sort of build-up and relaxation processes, we conclude that the direct problem solution, that is, modelling of precursory phenomena can be done just by using CP approach, neglecting the stationary ‘pure’ SOC component.

Of course, the inverse problem, the decomposition of the natural seismicity into stationary and non-stationary (precursory) components, is much more complicated. It is addressed in many papers (see, for example, Goltz 1997), but the problem is still far from the final solution.

## 2 PERCOLATION CRITICALITY MODEL

Percolation theory (Hammersley & Broadbent 1957; Stauffer & Aharony 1992; Sahimi 1994) was initially suggested to describe interaction of a fluid flow with a disordered medium, which can be imagined as a system of sites (or bonds). The transport properties of the disordered system depend on the concentration of inhomogeneities, such as a partial concentration,  $p$ , of being open for the flow sites. The increase of concentration of such sites results in formation of finite clusters, the number of which is  $N_{cl}$ . At the critical value  $p = p_c$ , that is, at the percolation threshold, which is the key parameter of the theory, finite clusters merge to form an infinite cluster (IC) that spans the whole system. The percolation process is described by several characteristic functions, for example, percolation probability,  $W(p)$ , the mean number of sites in a finite cluster,  $S(p)$  and the correlation length,  $R(p)$ , which depend mainly on the distance  $\Delta \varepsilon = (p - p_c)$  to the CP (Stauffer & Aharony 1992). That means that they can be considered as precursors of the formation of an IC.

The pure percolation model implies that there is no healing of damaged sites of the lattice, which corresponds to fracture of laboratory samples. In application to earthquakes, percolation can be considered as just one cycle of the seismic process. That means that fractures in the crust are healed after a strong earthquake. In prin-

ciple the healing can be implemented into the percolation model, using different approaches:

(i) The current concentration of damaged sites  $p$  can be considered as a difference between the cumulative content of damaged sites  $p_d$  less the content of healed sites  $p_h$ :  $p = p_d - p_h$ .

(ii) Annealing: in a finite system, which achieves an equilibrium state between nucleated and healed cracks, there is always a finite probability of IC formation at  $p_i$  less than but close enough to  $p_c$ . We can suppose that the number of damaged sites in a lattice is constant due to balance of nucleation and healing of defects. Besides, due to the random nature of locations of damaged and healed sites in the annealed model of percolation the configuration of the system of flaws is permanently changing. Some of these configurations allow IC formation; the probability of ‘rupturing’ configurations is higher for smaller system size and for greater damage  $p$ . According to the theory of Gaussian random processes, the probability of formation of IC in the range  $0 < p_i < p_c$  is (Levinstein *et al.* 1976):

$$N(p_i) \cong \Phi[(p_i - \langle p_c \rangle)/(D_p)^{1/2}], \quad (1)$$

where  $\Phi$  is the probability integral,  $\langle p_c \rangle$  is the average value of percolation threshold for a given size of lattice;  $D_p$  is the standard deviation of  $p_c$ :

$$D_p = B(\tilde{L} + C)^{-1/\nu} \quad (2)$$

Here  $B$  and  $C$  are constant,  $\tilde{L}$  is the size of the system in the lattice constant units,  $\nu$  is the critical index of correlation radius. Assuming that realization time of each new configuration is constant and equals  $T$ , one can find the average period of recurrence of rupture configuration, which is the analogue of seismic cycle duration (Chelidze 1982).

(iii) Newman & Turcotte (2002) suggested a hybrid model of seismic cycle, combining self-organized complexity (forest fire) and criticality (percolation) behaviour. A forest-fire component provides random occupation of sites (i.e. crack seeding and clustering). Due to tectonic stress the concentration of occupied sites grows up to the CP. When the IC spans the whole system; then all damaged sites, belonging to IC are removed (healed). The procedure simulates stress drop during a characteristic earthquake. After removing IC sites the free sites of lattice are again ‘planted’ with defects, till a new IC appears: that is a seismic cycle model.

In our opinion, the main component in the hybrid scheme is still the percolation model, which provides a CP of the process. The model does not differ much from the repeated percolation on the lattice, which became intact after attaining percolation threshold.

## 3 VALIDATION OF PERCOLATION MODEL OF FRACTURE (PMF)

The traditional theoretical models of fracture are either superlocalized as in linear fracture mechanics (LFM) (see Liebowitz 1984; Anderson 1991) or entirely delocalized as in (uniform) damage theory (Kachanov 1974; Bolotin 1998). During a real fracture process in heterogeneous solids we observe nucleation and coalescence of thousands of microcracks (Nolen-Hoeksema & Gordon 1987). That means that the LFM theory, which describes single crack behaviour, is not valid any more and besides, as microcracks are distributed rather inhomogeneously and form clusters of various sizes, the uniform damage theory also fails to be consistent with experiment.

What is the source of the fracture network complexity?

Experiments show that in composite solids the stress field is heterogeneous and contains local areas of elevated stress: it is enough to

consider experimental images or computer simulations of extremely complicated distribution of stresses in composite media, which are presented in the review of Meakin & Skjeltorp (1993, Figs 22 and 23) to understand that these images are not consistent with a memory-less SOC theory. It is clear also that microcracks nucleate at sites where the local stress exceeds the local strength. Thus a heterogeneous 'network' of stresses (Meakin & Skjeltorp 1993) transforms itself into a network of cracks (Nolen-Hoeksema & Gordon 1987), which has a strong memory, as the nucleated microcrack cannot be healed for a long time.

Another approach is developed in the kinetic theory of strength (Zhurkov *et al.* 1977). According to it, even in homogeneous solids the fracture will be delocalized due to the random breakage of atomic bonds visited by strong enough thermal fluctuations. The physical criterion of delocalization of fracture  $\beta$  is (Petrov 1979):

$$\beta = \frac{\alpha T}{3\varepsilon} \ln \tau / \tau_0, \quad (3)$$

where  $\alpha$  is the thermal expansion factor,  $T$  is temperature,  $\varepsilon$  is the limiting value of interatomic bond elongation,  $\tau$  is the sample durability and  $\tau_0$  is a constant for a given material. At  $\beta \rightarrow 1$  the fracture is delocalized and at  $\beta \rightarrow 0$  the process becomes highly localized (LFM domain).

Thus spatial and temporal heterogeneity of the stress field generates ramified fracture networks, which often form fractal structures (Chelidze & Gueguen 1990; Chelidze *et al.* 1994). These observations favour use of the percolation approach in the fracture analysis.

According to experimental data (Nolen-Hoeksema & Gordon 1987), the process of fracture of a heterogeneous solid develops in the following way: At first, isolated (single) microcracks appear in a solid. With an increasing load, or increased exposure time under constant load, the density of cracks increases. They begin to merge and at last, at a 'critical density of cracks', the main fracture is formed and transition from consolidated to unconsolidated state occurs. The concept of critical crack density was introduced by Scholz (1968), Brady (1974), Zhurkov *et al.* (1977); the latter formulated an empirical crack concentration criterion.

As the traditional theories of fracture are not consistent with the cited experimental data, a specific mathematical approach is needed to formalize the above qualitative physical models of the fracture process. The most general approach is a statistical topological description of fracture process in the framework of percolation theory, independent of the physical nature of elementary fracture nucleation.

A simple physical model of durable fracture (aging) corresponding to classical isotropic percolation theory can be built as follows. Let us consider a solid as a regular lattice of sites (or bonds) with characteristic size  $L$  and the lattice constant  $l$ . The elements of the lattice can either remain intact with probability  $p$  or be broken with a probability  $1-p$ . At first, all sites are intact, corresponding to an ideal intact solid. Then, at random, lattice sites 'spoil' one by one, as is postulated by the kinetic theory of multiple fracture (Zhurkov & Narzullaev 1953; Regel *et al.* 1974), according to which microcracks appear as a result of very large thermal fluctuations. As  $p$  increases, the solid lattice becomes more and more diluted. When dealing with lattices we assume that the effective size of elementary fracture is of order of lattice constant  $l$  and that only the nearest damaged elements (microcracks) can merge and form clusters (macrocracks). At the critical concentration of damaged elements  $p_c$  the IC of cracks, or a main rupture is formed, that is, disintegration of the body takes place. This value  $p = p_c$  is taken as the critical density of cracks that is sufficient for transition to the dy-

namical phase of fracture. The value of  $p_c$  is readily obtained either analytically or by computer simulations. The similarity of the physical phenomena with the percolation theory, of critical crack density with percolation threshold, and of the main fracture with an IC is readily apparent (Chelidze 1980a,b, 1982). A quite similar approach can be developed for forced fracture (Chelidze 1987, 1993).

Besides regular lattices it is possible to analyse the problem of random lattices, where the interaction range is not limited. In a simple 3-D case, when the bulk concentration of sites is  $N$  and each site has an interaction range  $R$  the theoretical condition of global connectedness of spheres, and consequently, of IC formation is (Pike & Seager 1974):

$$R_c/r_s = 1.4, \quad (4)$$

where  $r_s = 3/4(\pi N)^{1/3}$  is the mean distance between the sites at the concentration  $N$  and  $R_c$  is the critical value of interaction range, at which the IC of overlapping spheres is formed (Shante & Kirkpatrick 1971). On the other hand, experiments (Tamuž & Kuksenko 1978; Zhurkov *et al.* 1977) show that there exists an (empirical) crack concentration criterion, marking development of the main rupture, which practically coincides with the above percolation formulation (eq. 1). Namely, it was found that in the critical state the normalized mean distance between cracks is almost constant for various materials and for different scales of fracture process, from laboratory samples to tectonic faults:  $r_s/l \cong \text{const} \cong 4.5$ , where  $l$  is the mean size of the crack. This empirical rule is equivalent to the percolation transition criterion (eq. 4) at

$$R_c = 6l \quad (5)$$

(Chelidze 1986, 1987), which illustrates the agreement of the PMF with experimental data.

Percolation models are widely used for solution of problems of elasticity and fracture of damaged lattices (see, for example Herrmann & Roux 1990), especially at high concentrations of defects, when the traditional theory of elasticity of microheterogeneous solids (Hill 1965) cannot be applied.

Percolation theory can be used also to model the tectonic fault fracture (slip) process. In this case the fault is approximated by the random quasi-2-D percolation lattice, consisting of a system of asperities with fractal profiles, sliding one over the other. The tectonic stress initiates breaking (or plastic flattening) of the weakest asperities at first stages and failure of stronger ones at the following stages of fracture. We guess that the destruction of weakest asperities corresponds to the foreshock stage and the strong (characteristic) earthquake occurs when the critical number of asperities is broken. The statistics of the number of broken asperities can be transformed into statistics of waiting times at the asperities; then the critical number of broken asperities corresponds to the critical time (lifetime) of a system. This simplified kinetic approximation of fracture process allows connection of fractal fault rupture with a friction-mode interpretation of stick-slip process (Estrin & Brechet 1996). Thus the percolation model because of its universality can be applied to the fault fracture process also.

#### 4 ANISOTROPIC CORRELATION (AC)

There are physical processes (and one of them is the fracture percolation model) that require a simultaneous consideration of correlation and anisotropy. Correlation is due to the local stress field of an elementary crack that increases the probability of the new fracture occurrence in the vicinity of the existing one. The probability may also differ considerably in different directions due either to the action of external stresses or to the inherent anisotropy of the tested

material. These two effects lead to AC in the spatial distribution of microcracks.

Let the damage probability of the intact square lattice site depend on the state of its four nearest-neighbour sites and let  $p$  be the damage probability of the site, having no neighbouring populated sites. Let  $k$  be the parameter of correlation, showing how the population probability of the vacant site changes when it has a neighbouring populated site. To introduce AC, we determine two different correlation parameters  $k_h$  and  $k_v$  for two perpendicular directions. Then vacant sites with nine different population probabilities  $W_i$  may be present in the lattice. Since the total population probability  $\sum n_i W_i$  should sum to unity for all vacant lattice sites, we have (see for details Kolesnikov & Chelidze 1985):

$$\sum_{i=1}^{N_v} n_i W_i = 1, \quad (6)$$

where  $N_v$  is the number of vacant sites,  $n_i$  is a number of sites with the population probability  $W_i$ , which depends on the configuration of nearest damaged sites around the given vacant site:  $W_1 = p$  when all four neighbours are intact;  $W_2 = k_h p$  and  $W_3 = k_v p$  when only one neighbour site is damaged (here and below depending on additional site position we have different probabilities of occupation);  $W_4 = k_h^2 p$  and  $W_5 = k_v^2 p$  when two neighbours are damaged;  $W_6 = k_h k_v p$ ,  $W_7 = k_h^2 k_v p$  and  $W_8 = k_h k_v^2 p$  when three neighbours are damaged;  $W_9 = k_h^2 k_v^2 p$  when all four neighbours are damaged.

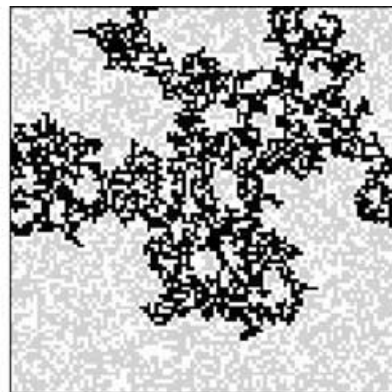
It is clear that when populating the lattice, the pattern of probability distribution over the vacant sites changes, and new probabilities

should be calculated according to (eq. 6) allowing for the changes in damage and cluster configuration. This procedure mimics redistribution of the stress field accompanying nucleation of defects.

## 5 PERCOLATION STRUCTURES

Typical structures of infinite percolation clusters on the square lattice (site model) at the percolation threshold for different values of AC coefficients are shown in Figs 1(a)–(c). Fig. 1(a) is characteristic for a non-correlated model, that is, for  $k_v = k_h = 1$ . Here and in the following figures the black pixels are for the IC and the grey ones show finite clusters. Fig. 1(b) shows the cluster structure for the case of positive (attractive) isotropic correlation ( $k_v = k_h = 10$ ) and Fig. 1(c) shows the same for the negative (repulsive) correlation ( $k_v = k_h = 0.1$ ). It is evident that strong attractive correlation promotes formation of dense clusters and that the percolation threshold in this case is achieved at a much larger concentration of damaged sites, excluding some low values of  $k$ , where  $p_c$  may be even less than in the case of  $k_v = k_h = 1$  (Duckers 1978).

Figs 2(a)–(d) shows cluster structures for anisotropically correlated percolation models at various combinations of AC coefficients  $k_v$  and  $k_h$ . The larger the difference between  $k_v$  and  $k_h$ , the less is the ramification of IC. The pattern of clustering depends not only on the absolute value of the ratio  $k_v/k_h$  but also on the absolute values of  $k_v$  and  $k_h$ : compare Figs 1(a) with (b) and (c) as well as Fig. 2a with Fig. 2c. It is evident that at the same ratio of  $k_v/k_h$  the damage pattern is different. The reason is that the absolute value of  $k_v$  (or



a.  $K_v=1, K_h=1$



b.  $K_v=10, K_h=10$  (attraction)



c.  $K_v=0.1, K_h=0.1$  (repulsion)

**Figure 1.** Structure of percolation clusters for isotropic models: (a) for  $k_v = k_h = 1$ ; (b) for  $k_v = k_h = 10$  (attraction) and (c) for  $k_v = k_h = 0.1$  (repulsion). On Figs 1 and 2 the grey pixels show finite clusters; the black ones delineate the infinite cluster.

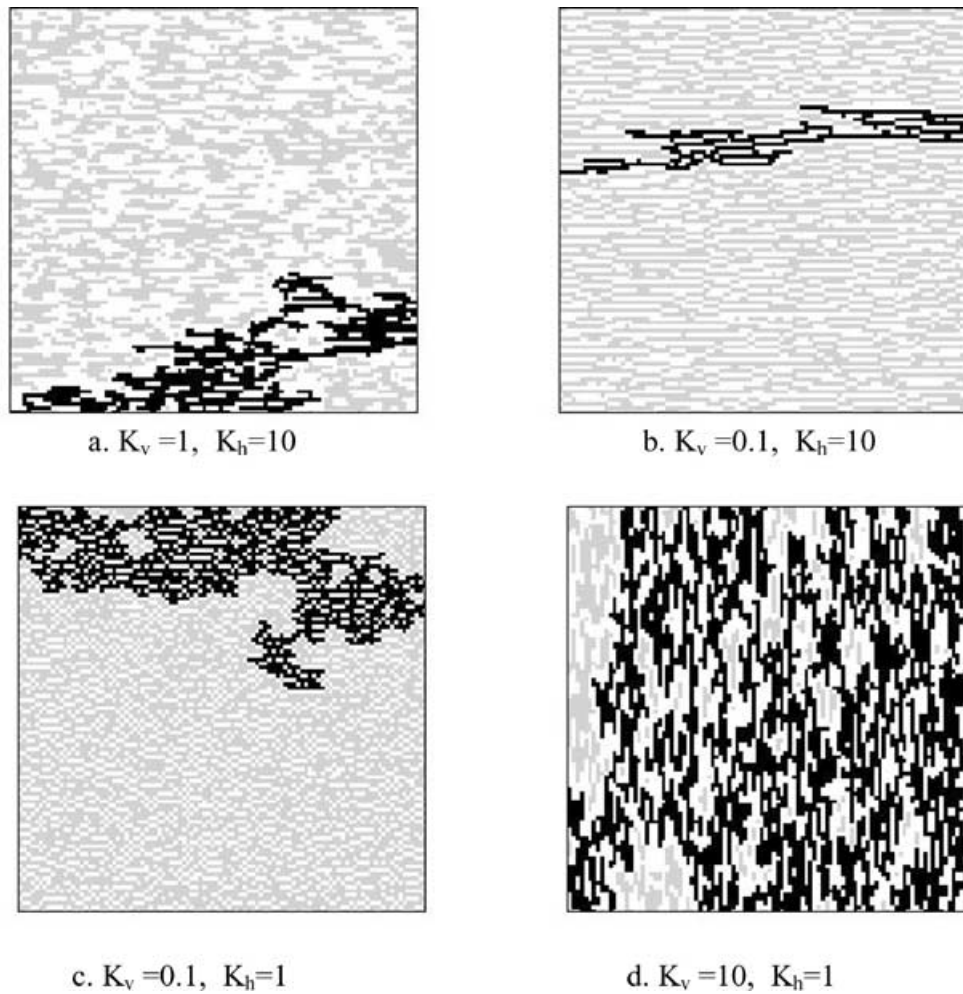


**Figure 2.** Structure of percolation clusters for anisotropically correlated models: (a) for  $k_v = 1$  and  $k_h = 10$ ; (b) for  $k_v = 0.1$  and  $k_h = 10$ ; (c) for  $k_v = 0.1$  and  $k_h = 1$  and (d) for  $k_v = 10$  and  $k_h = 1$ .

$k_h$ ) stipulates either attractive or repulsive correlation at clustering and correspondingly affects the geometrical pattern of the fracture network as well as all percolation functions. When one of the correlation coefficients is much larger than the other one (Fig. 2c), the IC tends to the linear form, that is the PMF is actually reduced to the case of LFM (Kolesnikov & Chelidze 1985). Actually, any real crack network can be reproduced theoretically by the proper choice of percolation model (for example, the growth model, used by Sawada *et al.* 1982) and a realistic approximation of physical interaction of sites, say, by various AC coefficients (Cowie *et al.* 1993; Renshaw & Pollard 1994; Chelidze 1993). It is interesting to compare our results with numerical and physical simulation of fracture set formation performed by Renshaw & Pollard (1994). The modelling was aimed to relate geometric aspects of natural fracture patterns to the stress state operating during their formation. After specification of the initial flaws' geometry they were subjected to a constant remote stress; for each flaw a stress intensity factor (SIF)  $K$ , representing the degree of stress concentration at the crack tip was calculated. The flaws with SIF greater than the critical value were advanced in a straight line over a distance  $l_a$ , proportional to  $K$ :

$$l_a \cong 2a \left[ \frac{(1 - \nu^2)E}{(1 - \nu_c^2)E_c} \right]^\alpha \left( \frac{K_I}{K_{Ic}} \right)^\alpha, \quad (7)$$

where  $a$  is grid spacing,  $\nu$  is Poisson's ratio,  $E$  is Young's modulus and  $\alpha$  is the flaw growth velocity exponent; the subscript  $c$  corresponds to the situation when the SIF approaches the critical value. We consider  $\alpha$  as a proxy of our AC coefficient because the increase of both these parameters stimulates the directed growth of a flaw. The fracture patterns obtained by Renshaw and Pollard are very similar to those shown in Figs 1 and 2, but their conclusion that the extent of fracture clustering is not very sensitive to the flaw density (parameter  $p$  in percolation model) is not consistent with our results.

## 6 ENERGY EMISSION MODEL

Nucleation and coalescence of defects implies some energy emission, as each such act causes redistribution of local stresses. A model of elastic wave emission and amplitude distribution during failure was first suggested in (Chelidze & Kolesnikov 1984). This assumes that the emergence of each new defect is associated with an emission event and that the (conventional, effective) emission amplitude  $A$  generated by the addition of a single elementary event depends directly on the increment of the size of the resulting (offspring) defect cluster induced by this event. In contrast to other models, where the total number of finite clusters is considered as a proxy of emitted energy pulses (earthquakes), we presume that emission occurs only when the increment of the size of merging clusters of defects

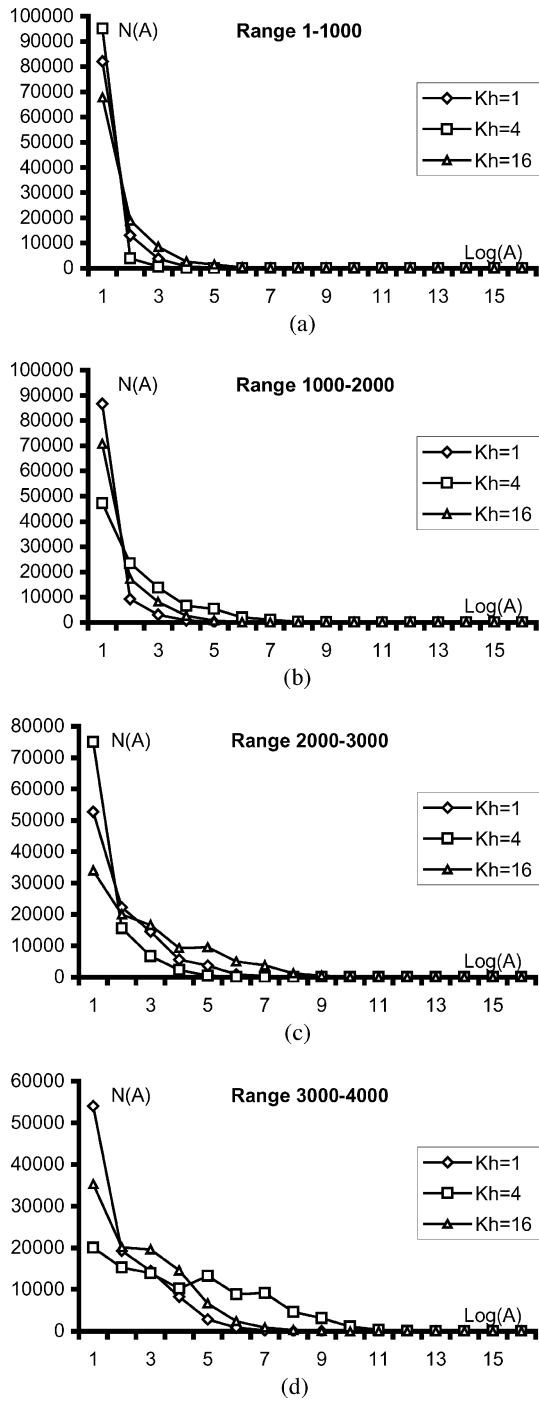


**Figure 3.** Dependence of number of events of a given effective amplitude  $A$  versus logarithm of amplitude (discrete frequency–magnitude plot) for various anisotropic correlation factors ( $k_h = 1, 4, 16$  at  $k_v = 1$ ) and different intervals of damage: (a) 1–1000; (b) 1000–2000; (c) 2000–3000; (d) 3000–4000; (e) 4000–5000 and (f) 5000–6000. The lattice is  $100 \times 100$ , the data are averaged over 100 runs.

takes place. This assumption is quite natural, as the clusters, which do not change at all at the addition of an elementary defect, should not emit energy. For this model of ‘active clusters’ the effective (conditional) emission amplitude  $A_c$ , generated by each elementary fracture depends directly on the increment of the size of the resulting (offspring) cluster of defects, induced by the addition of a single

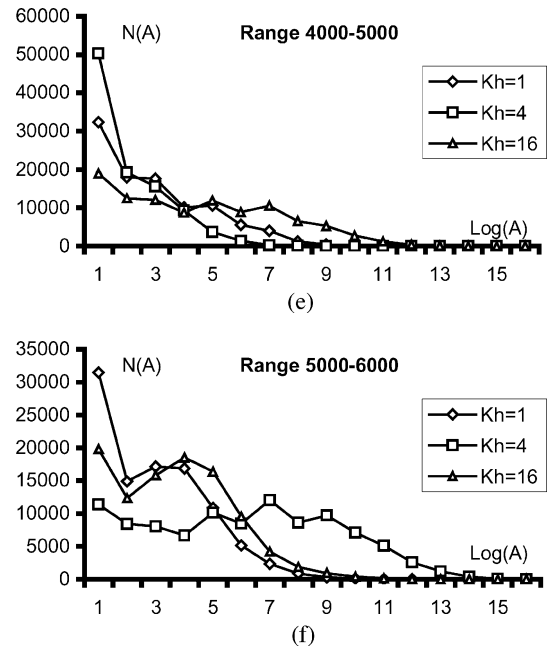


**Figure 3.** (Continued.)

defect (Chelidze & Kolesnikov 1984):

$$A = A_0 \left( \left( \sum_{i=1}^{k+1} s_i \right)^2 - \left( \sum_{i=1}^k s_i^2 \right) \right)^{1/2}, \quad (8)$$

where  $k$  is the number of clusters linked by the elementary defect,  $s$  is the number of sites in the  $i$ th merging cluster, and  $A_0$  is a conventional amplitude, generated by the nucleation act of a single isolated defect. Implicitly  $A_0$  takes into account the elastic moduli  $M$  of the system  $A_0 = f(M)$ . For the present  $A_0$  is considered constant. This probably is not true for the last stages of fracture, as the elastic modulus of the damaged solid is a function of damage  $p$  (Sahimi 1994; Chelidze *et al.* 1998). A theoretical expression for energy emission  $\Delta E$  at the addition of one damaged site, expressed by means of fundamental percolation functions, is given in (Chelidze 1986), where  $\Delta E$  is calculated as a derivative of the mean size of finite clusters is:

$$\begin{aligned} \Delta E &= \frac{d}{dp} \sum_s s^2 n_s(p) \Big/ \sum_s s n_s(p) \\ &= p \frac{ds(p)}{dp} + s(p) = \left( \sum_{i=1}^{k+1} s_i \right)^2 - \left( \sum_{i=1}^k s_i^2 \right), \end{aligned} \quad (9)$$

where  $n_s$  is the number of clusters of size  $s$  and at differentiating we take into account that for  $p < p_c$  the sum  $\sum_s s n_s(p) = p$ . For  $p \rightarrow p_c$  we get:

$$\Delta E \approx |p - p_c|^{-(\nu+1)} = s(1 + L_R), \quad (10)$$

where  $L_R$  is the average number of cutting (‘red’, single) bonds in an incipient IC (Chelidze & Kolesnikov 1984). The same approach has been used by Sammis & Sornette (2002) and they obtained similar expressions for  $\Delta E$ .

In our earlier paper we calculated the amplitude distribution for the case of isotropic percolation (Chelidze & Kolesnikov 1983, 1984). Here we are presenting new results, obtained on larger lattices and for anisotropically correlated percolation processes. In Figs 3(a)–(f), the evolution of amplitude distribution during the fracture process on a square lattice  $100 \times 100$  (site model) for three

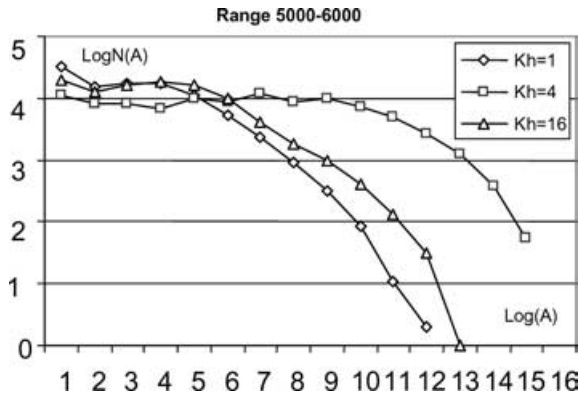


**Figure 4.** The log–log plot of dependence of number of events of amplitude  $A$  versus amplitude close to  $p_c$  for various anisotropic correlation factors ( $k_h = 1, 4, 16$  at  $k_v = 1$ ). The lattice is  $100 \times 100$ , the data are averaged over 100 runs.

different values of  $k_h = 1, 4, 16$  and  $k_v = \text{const} = 1$  is presented. The values of amplitude  $A$  in all plots are in relative units of ‘elementary amplitude’  $A_0$ . The numbers on the plots indicate the range of damage probability  $p$ . The  $p = 0.6$  corresponds to the isotropic percolation threshold of the square lattice. The particular behaviour of the curves for  $k_h = 4$  can be explained by a clustering peculiarity at this value of correlation factor: the percolation threshold is minimal for correlation coefficients 4–5 (Duckers 1978).

The character of discrete plot of the number of events  $N$  of amplitude  $A$  (i.e. of the quantity  $N(A)$ ) versus  $\log A$  changes drastically in the interval of damage  $p$  from 0.3 to 0.4, where instead of monotonic decrease of  $N(A)$  with increase of  $\log A$  that we see at lesser damage, the  $N(A)$  curves manifest complicated behaviour with plateaus and maxima. That means that close to the percolation threshold (critical state) there are some characteristic values of  $A$ , which are encountered much more frequently than other values. It is interesting to note that Renshaw & Pollard (1994, Fig. 10) also obtained a maximum in the average fracture length distribution at the advanced stages of their numerical simulations of fracture networks, which can be compared with our results on the existence of preferable values of  $A$  close to the percolation threshold. Fig. 4 shows the log–log plot of dependence of number of events of amplitude  $A$  versus amplitude close to  $p_c$  for various AC factors ( $k_h = 1, 4, 16$  at  $k_v = 1$ ). Both semi-logarithmic and log–log plots (Figs 3 and 4) reflect the fact that there is a characteristic (preferable) amplitude in the frequency–amplitude distribution, which becomes evident as a bump in some range of damage (see also Main 1992).

Our results confirm the view that events with large effective amplitudes should occur in some range of damage more frequently than is predicted by linear interpolation of the frequency–magnitude relation from the low magnitude domain. The bump in the discrete frequency–amplitude plot (Figs 3c–f) reflects the crossover in clustering mode connected with the correlation length  $\xi$ , which can be loosely defined as the radius of clusters, which give the main contribution to the characteristic percolation functions (mean cluster size, etc.). Thus, close to  $p_c$  the (average) mass of clusters within a box of size  $L$  for  $L < \xi$  obeys a power-law  $M(L) \propto L^D$ , where  $D$  is the fractal dimension of the clusters, and at  $L > \xi$  the mass  $M$  is practically constant; at  $L > 2\xi$  the mass decreases drastically. We guess that the increment of the mass of cluster, which is a proxy to effective amplitude, depends on  $L$  in a similar way.

Numerical experiments on lattices of various sizes show that the larger is the lattice edge size  $L$ , the larger is the maximal effective

amplitude  $A_{\text{max}}$ , which corresponds to the percolation threshold; the  $A_{\text{max}}$  value increases very fast at large  $L$ .

In order to reveal possible non-linear structure in the sequence of (percolation) effective amplitudes they were analysed using the Lempel-Ziv (LZ) complexity test. LZ complexity of a coded sequence of the length  $N$  is defined as (Lempel & Ziv 1976; Sprott & Rowlands 1995):

$$C_{LZ} = \lim_{N \rightarrow \infty} \frac{L(N)}{N}, \quad (11)$$

where  $L(N)$  is the length of a coded sequence. LZ complexity characterizes the compressibility of a sequence/time-series. If the sequence is quite random, it is incompressible and the length of the encoded sequence  $L(N)$  equals the length of the whole sequence  $N$ , so  $LZ = 1$ . Existence of some ordered patterns (matches) allows compression of data, the length of the encoded sequence decreases and correspondingly  $LZ < 1$ . For example, LZ of a sine function is close to zero. This method has practically no restrictions in terms of the length of the time-series and is valid even for short (300–400 point) data length sequences.

It is intriguing that the LZ complexity of effective amplitude sequences,  $LZ = 0.750$ , is significantly less than LZ for a random process ( $LZ = 1$ ). Besides, Hurst exponents for these sequences are in the range 0.8–0.85. Both these results point to the appearance of some order in the generation of effective emission events, due, probably, to the memory property of the percolation process. This structure is not observed in a sequence of random numbers, used for percolation simulations and generated by a random number generator.

## 7 PREDICTIVE SIGNS IN PERCOLATION MODEL

Besides providing a theoretical framework for description of fracture source evolution, the PMF opens the possibility to elaborate predictive signs of final rupture based on the first principles of percolation theory. Such precursors are (Chelidze 1986):

- (i) attaining the critical concentration of fractures  $p_c$ ;
- (ii) divergence of finite size of clusters  $s$ , correlation length  $L_c$  and effective amplitudes as power-law of  $(p - p_c)$  at  $p \rightarrow p_c$ ;
- (iii) strong increase of number of large pulses;
- (iv) strong increase in the scatter of amplitudes and
- (v) decrease of slope of magnitude–frequency relation.

Many of these precursors have been observed in the laboratory and in field data (Chelidze 1982, 1986; Sobolev 1993; Tamuž & Kuksenko 1978). Here we try to reveal some predictive signs of closeness to the CP in the series of effective amplitudes emitted during the percolation process.

On Fig. 5(a) is shown the cumulative curve (analogue of Benioff curve) of  $A$  versus number of damaged sites  $N$  for a single run on the  $30 \times 30$  lattice for a non-correlated percolation process; Fig. 5(b) presents the averaged curve for 100 runs. The dependence  $A(N)$  for the individual run manifests a clear transition from a smooth increase till  $N \cong 550$  to a complicated behaviour with jumps. The large jumps correspond to strong events and the largest one at  $N = 600$  marks the percolation threshold. The average for 100 runs  $A(N)$  curve (Fig. 5b) is quite smooth so that it is not possible to recognize the approaching percolation transition, but even on the averaged curve there are deviations from the average (Fig. 5c) that increase drastically close to  $p_c$ , that is close to  $N = 600$ .

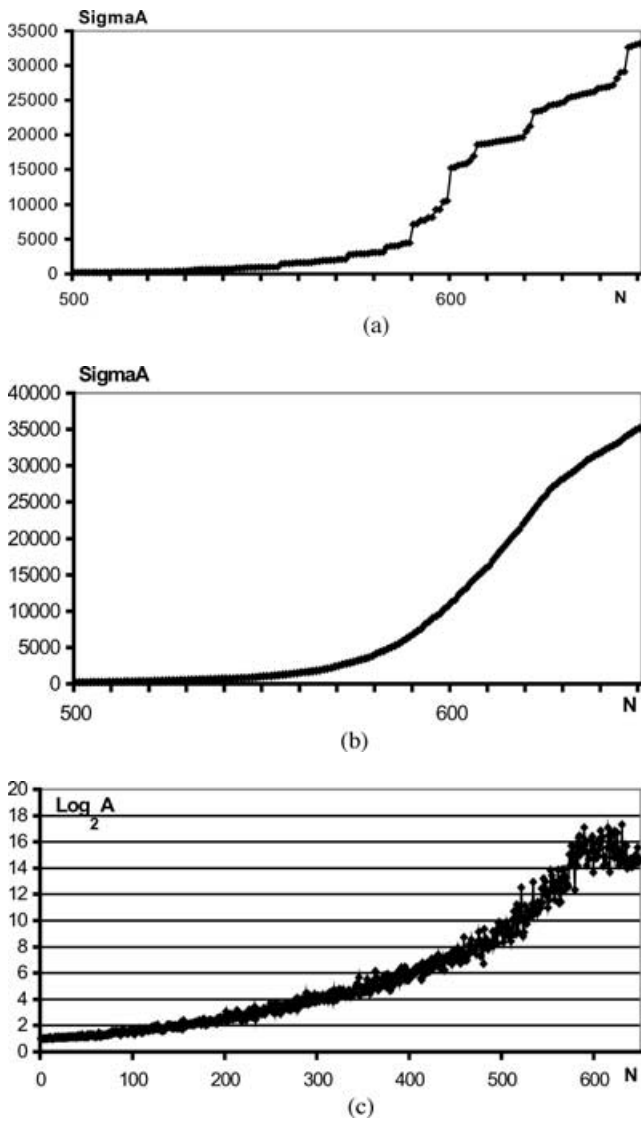


**Figure 5.** (a) Cumulative graph of amplitude (Sigma  $A$ ) versus number of damaged sites  $N$  for a single run (lattice  $30 \times 30$ )—analogue of Benioff curve;  $p_c = 0.67$  or  $N = 600$ . (b) Cumulative graph of amplitude (Sigma  $A$ ) versus number of damaged sites  $N$  averaged for 100 runs (lattice  $30 \times 30$ );  $p_c \approx 0.65$  or  $N \approx 600$ . (c) Cumulative graph of amplitude versus number of damaged sites  $N$  for 100 runs in semilogarithmic scale (lattice  $30 \times 30$ );  $p_c \approx 0.65$  or  $N \approx 600$ . Note increase in (averaged) scatter close to  $p_c$ .

Fig. 6(a) presents the cumulative amplitude  $\Sigma A$  versus number of defects for various AC coefficients ratio  $r_{AC}$  ( $r_{AC} = 1, 4, 16$ ). It seems that at the same damage  $N$  the emission is most pronounced for large values of  $r_{AC} = 16$ , and the large amplitudes ( $A > 1000$ ) appear much earlier at large values of  $r_{AC} = 16$ , which is quite natural as far as correlation promotes formation of large clusters. At the same time if we rescale the plots in units of  $p/p_c$  the behaviour of  $\Sigma A$  near the percolation threshold is opposite to the previous one: the minimal values of  $\Sigma A$  at  $p/p_c = 1$  are obtained for strong AC and maximal ones correspond to the isotropic model (Fig. 6b). This is due to the decrease of percolation threshold in AC models. In other words the IC in AC percolation appears at much less damage (much less acts of emission) than in the isotropic model.

As the prediction of a single earthquake cannot be made on the basis of statistically averaged data, the analysis of scatter was per-

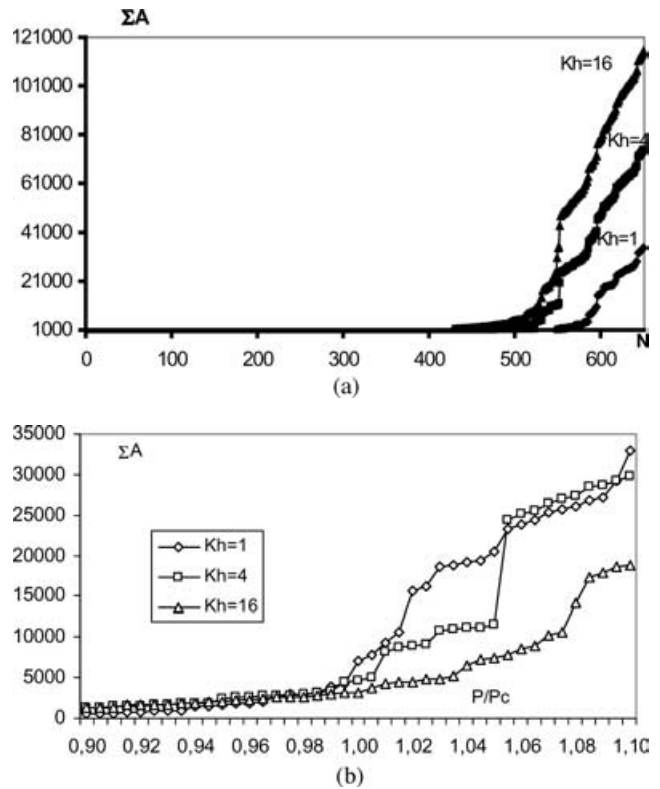


**Figure 6.** Cumulative graph of amplitudes larger than 1000 (Sigma  $A > 1000$ ) versus number of damaged sites  $N$  for a single run at different correlation factors  $Kh = 1, 4, 16$  (lattice  $30 \times 30$ ); note that for  $Kh = 1$   $P_c = 0.586$ , for  $Kh = 4$   $P_c = 0.524$  and for  $Kh = 16$   $P_c = 0.491$ .

formed for an individual percolation run as well as for 1, 10, 100 and 1000 runs (compare Figs 7a–d). Here we used ‘interval’ or ‘moving’ averages of amplitude and amplitude-scatter parameters (dispersion) in successive 100-elementary-event windows during the percolation process, in order to analyse the behaviour of the above parameters and to establish their validity as precursors of failure. The percolation threshold is in the range 0.5–0.6. It is evident that even in the individual run, close to the percolation threshold the dispersion amplitudes  $D_a$  in a sequence of 100-events windows increases immensely and the slope of  $\log D_a$  increases significantly (Fig. 7a). This crossover in the slope can be considered as a precursor of the CP. What is more, the ‘scatter precursor’ works much better in the case of an individual run than for repeated runs. Thus, the drastic increase in the scatter of amplitudes in consecutive 100-events windows (we can call it ‘interval scatter’) is a good precursor of the impending critical state, as was predicted in (Chelidze 1986). That is why the ‘scatter precursor’ is preferable:  $D_s$  deviates from the background line much earlier and more strongly than the amplitude plot. The amplitude acceleration effect becomes very strong only for large statistics (Fig. 7d) which is unrealistic in the study of natural seismic processes.

It is interesting to consider the problem of maximal amplitude of the eventual strongest event (earthquake) in the percolation model. It is evident that the strongest event is generated by the maximal increment of the size of the resulting cluster that is with formation of the IC, which means that the maximal possible amplitude will be defined by the size of the lattice  $L$ . That is similar to an assessment of maximal possible earthquake by the size of the fault.



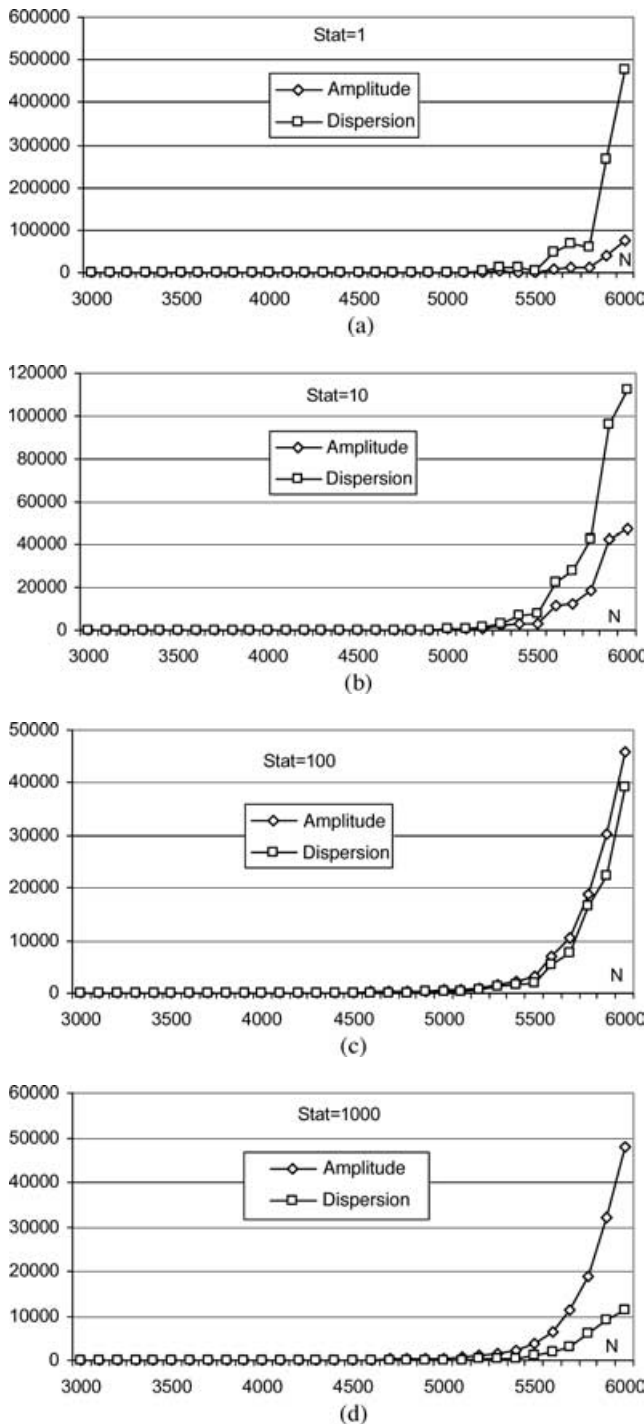


Figure 7. Dispersion of amplitudes and the mean value of amplitudes in consecutive windows, containing 100 events versus number of damaged sites for a single run (stat = 1, Fig. 7a) and for statistics 10, 100 and 1000 (correspondingly, Figs 7b–d); isotropic percolation model.

### 8 TIME-TO-FAILURE IN PERCOLATION MODEL

The original percolation theory considers the sequence of elementary events without any reference to the time domain. In order to introduce time dependence into percolation it is necessary to assert some kinetic conjectures. In our first papers (Chelidze 1980a,b,

1982) as well as in many others (Meakin & Skjeltorp 1993; Main 1999) each defect nucleation act was considered as demanding the unit time step. Such a hypothesis on the constant rate of defect nucleation is undoubtedly an oversimplification (Chelidze 1987, 1993), but it can be accepted as a first approximation.

It has been shown (Chelidze 1980, 1982) that many time-dependent precursors  $P(t)$  of failure of solids and earthquakes can be approximated as a power-law dependence on the ‘temporal distance’ to the moment of final rupture  $t_f$ :

$$P(t) \propto (t_f - t)^m, \tag{12}$$

where  $t$  is the current time and  $m$  is the constant.

The same conclusions follow from the latest works (Voight 1988, 1989; Main 1999). I. Main shows that three different models: subcritical crack growth, Voight’s approach and PMF predict the power-law expressions for the time-to-failure, similar to (eq. 12).

Several physically reasonable approaches for implementing more realistic time dependence of damage in PMF are suggested in (Chelidze 1986, 1987). The most realistic is to admit the universal kinetic law of reliability theory (Gnedenko 1965), which can be approximated by the double Weibull distribution for the damage rate probability  $P(t)$ :

$$P(t) = 1 - [K \exp(-c_1 t^\alpha) + (1 - K) \exp(-c_2 t^\beta)], \tag{13}$$

where  $0 < \alpha < 1$ ,  $\beta > 1$ ,  $0 < K < 1$ ,  $t$  is changing between 0 and 1 (1 corresponds to the moment of final rupture);  $c_1$  and  $c_2$  are positive constants. For such a distribution the intensity of elementary acts of failure  $P$  first decreases due to burning of weak elements of the system and then, after a long period of relative quietness that makes up the main part of the sample’s longevity,  $P$  sharply increases (which corresponds to the acceleration phase in the CP approach). For  $t \rightarrow 1$  and small  $\beta$  the last term tends to a power-law expression (Gvishiani & Dubois 2002), similar to (12).

The kinetic theory of strength of solids, which reveals the physical nature of durability, is developed in (Zhurkov & Narzullaev 1953; Regel *et al.* 1974; Tamuž & Kuksenko 1978).

### 9 ACCELERATION MODEL TESTS ON PERCOLATING SYSTEMS

It is interesting to compare the behaviour of the effective amplitude  $A$  in the PMF with predictions of the criticality theory on the accelerating rate of seismicity before a strong event.

Considering a time-series of events of given amplitude  $A$ , as a model for seismic process energy release, it is necessary to decide which of these time-series correspond to the seismic regions with higher and/or lower level of accelerated energy release. For this purpose curvature parameter analysis following Bowman *et al.* (1998) has been carried out on percolation models (lattices  $100 \times 100$ ) at various AC factors  $k_h$ ; the value of  $k_v$  was kept constant,  $k_v = 1$  (Fig. 8). The curvature parameter  $C$  is deduced from the Benioff strain  $E(t) = \sum_{i=1}^{N(t)} E_i(t)^{1/2}$ , where  $E_i$  is the energy (here  $A$ ) of the  $i$ th event, as a relative quality of power-law/linear fitting of dependence of cumulative energy release against time and is defined as  $C = \text{power-law rms/linear rms}$ .

Generally for accelerating sequences  $C < 1$  and for decelerating sequences  $C > 1$ .

As follows from Fig. 8, the curvature parameter of mentioned time-series permanently decreases when  $k_h$  increases. The significant decrease of curvature parameter for amplitude time-series with large AC factors indicates that energy release acceleration rate increases at larger  $k_h$ .

Curvature parameter of cumulative amplitudes for various anisotropic correlation factors

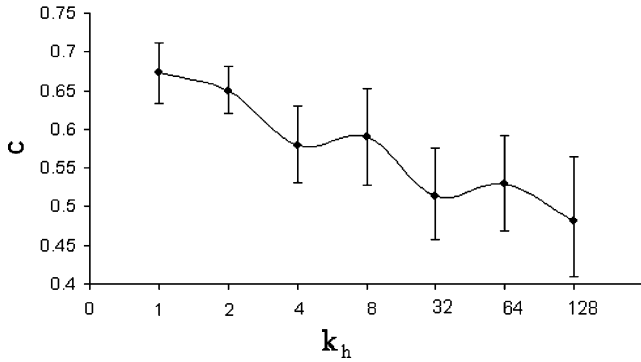


Figure 8. Curvature parameters of amplitude time-series at various anisotropic correlation factors  $k_h$ .

Power law fit error of cumulative amplitudes for various anisotropic correlation factors

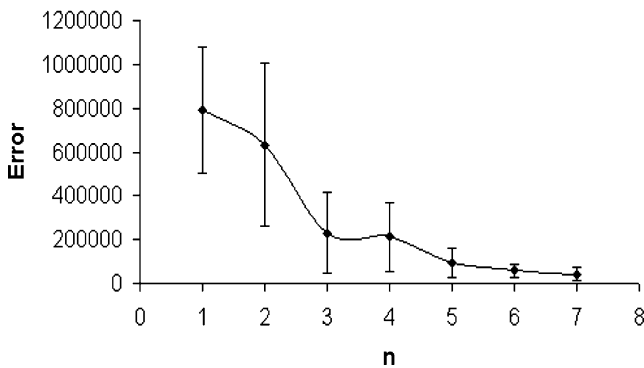


Figure 9. Power-law fit error of amplitude time-series at various anisotropic correlation factors.

In order to verify this important (but somewhat ambiguous due to essential calculation error), conclusion for further analysis we have also used another reliability testing procedure. Namely, as shown in Fig. 9, the error of power-law fitting also significantly decreases at larger values of AC factor  $k_h$ . Moreover, the coefficient of multiple determination, a characteristic of quality of fitting, notably increases when  $k_h$  increases.

These results clearly indicate that amplitude time-series for larger AC factors ( $k_h > 4$ ) can be considered as a model of critical seismic region with strongly accelerated energy release, ending with a the strong earthquake. In principle, this conclusion is in agreement with well-known seismic process models (Miachkin *et al.* 1975; Sobolev 1993), which predict localization of fracture in the incipient (anisotropic) fault zone.

### 10 SHANNON ENTROPY OF EFFECTIVE AMPLITUDE SEQUENCES

In recent years the concepts of thermodynamics such as information entropy have been applied to the analysis of seismic processes in order to analyse proximity to criticality (Main & Al-Kindy 2002; Al-Kindy & Main 2003). As far as the decrease of the curvature parameter corresponds to increased clustering, we assume that a potentially critical region with accelerated energy (amplitude) release

Shannon entropy of amplitude time series versus intervals of damage and various correlation factors

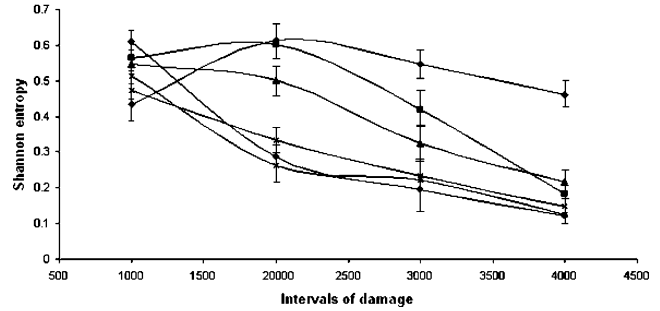


Figure 10. Shannon entropy of amplitude time-series for different damage intervals. Shannon entropy for values of  $k_h = 1$  (diamonds), 8 (squares), 16 (triangles), 32 (crosses), 64 (stars) and 128 (circles) are shown sequentially. Error bars show standard deviation for the same events sequence of shifted windows, containing the same number of events.

Shannon entropy of cumulated amplitude time series versus intervals of damage and various correlation factors

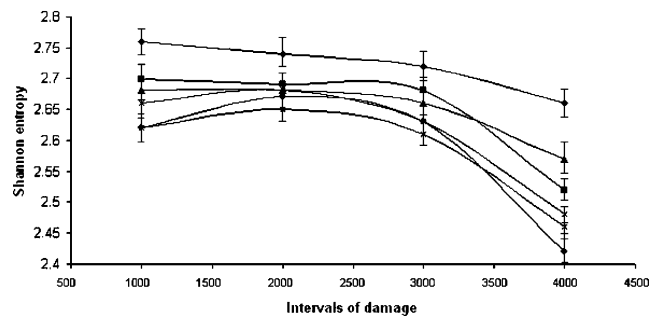


Figure 11. Shannon entropy of cumulated amplitude time-series for different damage intervals. Shannon entropy for values of  $k_h = 1$  (diamonds), 8 (squares), 16 (triangles), 32 (crosses), 64 (stars) and 128 (circles) are shown sequentially. Error bars show standard deviation for the same events sequence of shifted windows, containing the same number of events.

may also have lower value of Shannon entropy at short timescales before the strongest event. The Shannon entropy calculation is based on analysis of the probability distribution, and is not restricted by the type of analysed dynamics. In the present paper Shannon entropy  $S = -\sum_{i=1}^N P_i \log(P_i)$ , where  $P_i$  is the probability of an event occurring within the  $i$ th box, was calculated for the analysed time-series.

It was found earlier that magnitude sequences of large Caucasian earthquakes (opposite to spatial and temporal domains) are mostly characterized by the decrease of Shannon entropy (Matcharashvili *et al.* 2002).

As shown in Fig. 10, amplitude time-series that model more ‘anisotropic’ critical regions (i.e. series with  $k_h > 4$ ) indeed reveal clear permanent decrease of Shannon entropy for short time periods (damage intervals) before strong earthquake (percolation threshold), unlike time-series at lower values of AC factors.

In order to verify the obtained results and avoid errors, which may be expected with probability calculations of spiked data, we also carried out a Shannon entropy variation test on the cumulated data sets (Fig. 11). It is evident that the tendency of decrease is well outside of error range.

From the above it is possible to suppose that a permanent decrease of SE value of the magnitude distribution (or an increase of extent

of order in the dynamics of the released energy distribution) may be considered as a characteristic feature for regions of stronger AC, hence, a smaller waiting time to the forthcoming earthquake, as the percolation threshold is achieved at lesser damage. In general, the decrease of SE value can be considered as a predictive sign.

## 11 CONCLUSIONS

We considered the anisotropically correlated PMF as an example of CP approach to evolution of the seismic process. The geometry of fracture structures, energy emission distribution and evolution of scatter of emitted amplitudes at attaining the CP (percolation threshold) are analysed. It is shown that a drastic increase in the scatter of amplitudes is a good precursor of the impending CP. The LZ complexity test reveals clear non-linear structure in the sequence of effective amplitudes; the value  $LZ = 0.750$  is significantly less than LZ for a random process ( $LZ = 1$ ) and the Hurst exponent is in the range 0.8–0.85. Both these results point to the appearance of some order in generation of effective emission events, due, probably, to the memory property of the percolation process. Various tests (curvature parameter, Shannon entropy and coefficients of multiple determination) show that the acceleration of model seismicity close to the CP increases with the growth of AC.

## ACKNOWLEDGMENTS

This work was supported by INTAS grant 01-0748, 2002. The authors are grateful to the reviewers for useful remarks.

## REFERENCES

- Al-Kindy, F. & Main, I., 2003. Testing self-organized criticality in the crust using entropy: a regionized study of the GMT global earthquake catalogue, *J. geophys. Res.*, **108B**, ESE 5 (1–9).
- Allegre, C., Le Mouell, J. & Provost, A., 1982. Scaling rules in rock fracture and possible implications for earthquake prediction, *Nature*, **297**, 47–49.
- Anderson, T., 1991. *Fracture mechanics: Fundamentals and Applications*, CRC Press, Boca Raton.
- Bak, P., Tang, C. & Wiesenfeld, K., 1988. Self-organized criticality, *Phys. Rev. A*, **38**, 364–374.
- Bolotin, V.V., 1998. *Mechanics of Fracture*, CRC Press, Boca Raton.
- Bowman, D., Ouillon, G., Sammis, C., Sornette, A. & Sornette, D., 1998. An observational test of the critical earthquake concept, *J. geophys. Res.*, **103**, 24 359–24 372.
- Brady, B.T., 1974. Theory of earthquakes, *Pure appl. Geophys.*, **112**, 701–714.
- Chelidze, T., 1980a. The model of fracture process of solids, *Solid State Physics (Moscow)*, **22**, 2865–2866 (in Russian).
- Chelidze, T., 1980b. Theory of percolation and fracture of rocks, in *Proceedings of VI All Union Conference on mechanics of rocks, Frunze, 1978*, pp. 107–117 (in Russian).
- Chelidze, T., 1982. Percolation and fracture, *Phys. Earth planet. Inter.*, **28**, 93–101.
- Chelidze, T., 1986. Percolation theory as a tool for imitation of fracture process in rocks, *Pageoph*, **124**, 731–748.
- Chelidze, T., 1987. *Percolation Theory in Mechanics of Geomaterials*, Nauka, Moscow, p. 273 (in Russian).
- Chelidze, T., 1993. Fractal damage mechanics of Geomaterials, *TerraNova*, **5**, 421–437.
- Chelidze, T., 2000. Earthquake prediction: pro and contra, in *Earthquake Hazard and Seismic Risk Reduction*, pp. 225–229, eds Balassanian, S., Cisternas, A., Melkumyan, M., eds, Kluwer, Netherlands.
- Chelidze, T. & Gueguen, Y., 1990. Evidence of fractal fracture, *Int. J. Rock Mech. Min. Sci.*, **22**, 223–225.
- Chelidze, T. & Kolesnikov, Yu., 1983. Modelling and prognosis of fracture process within framework of percolation theory, *Izvestia AN SSSR, Physics of Earth, N 5*, 24–34.
- Chelidze, T. & Kolesnikov, Yu., 1984. On the physical interpretation of transitional amplitude in percolation theory, *J. Phys. A*, **17**, L791–L793.
- Chelidze, T., Reushle, T., Darot, M. & Gueguen, Y., 1988. On the elastic properties of depleted refilled solids near percolation, *J. Physics C*, **21**, L1007–L1010.
- Chelidze, T., Reuschle, T. & Gueguen, Y., 1994. A theoretical investigation of the fracture energy of heterogeneous brittle materials, *J. Phys. Cond. Matter*, **6**, 1857–1868.
- Chelidze, T., Gueguen, Y. & Le Ravalec, M., 1998. From classic to fractal mechanics of disordered media; self-consistency versus self-similarity, in *Probamat-21st Century; Probabilities and Materials*, pp. 197–231m, ed. Frantzikonis, G.N., Kluwer, Netherlands.
- Cowie, P., Vanneste, C. & Sornette, D., 1993. Statistical physics model for the spatio-temporal evolution of faults, *J. geophys. Res.*, **98**, 21 809–21 821.
- Duckers, L., 1978. Percolation with nearest neighbour interaction, *Phys. Lett. A*, **67**, 93–94.
- Estrin, Y. & Brechet, Y., 1996. On a model of frictional sliding, *Pageoph.*, **147**, 745–762.
- Gnedenko, B., 1965. *Mathematical methods of reliability theory*, Nauka, Moscow, p. 524 (in Russian).
- Goltz, C., 1997. *Fractal and chaotic properties of earthquakes*, Springer, Berlin, p. 175.
- Gvishiani, A. & Dubois, J., 2002. *Artificial Intelligence and Dynamic Systems for Geophysical Applications*, Springer, Berlin, p. 347.
- Hammersley, L. & Broadbent, J., 1957. Percolation processes, *Proc. Cambridge Philos. Soc.*, **53**, 269–290.
- Herrmann, H. & Roux, S. (eds), 1990. *Statistical Models for the Fracture of Disordered Media*, North-Holland, p. 353.
- Hill, R., 1965. A self-consistent mechanics of composite materials, *J. Mech. Phys. Solids.*, **13**, 213–223.
- Huang, Y., Saleur, H., Sammis, C.G. & Sornette, D., 1998. Precursors, aftershocks, criticality and self-organized criticality, *Europhys. Lett.*, **41**, 43–48.
- Kachanov, L.M., 1974. *Fundamentals of Fracture Mechanics*, Nauka, Moscow, (in Russian).
- Kolesnikov, Yu. & Chelidze, T., 1985. The anisotropic correlation in percolation theory, *J. Phys. A*, **18**, L273–L275.
- Lempel, A. & Ziv, J., 1976. On the complexity of finite sequences, *IEEE Transactions on Information Theory*, **IT-22**(1), 75–81.
- Levinstein, M., Shur, M., Shklovsky, B. & Efros, A., 1976. On connection between critical indices of percolation theory, *Jour. Exper. Theor. Physics (Russia)*, **69**, 386–392 (in Russian)
- Liebowitz, H. (ed.), 1984. *Fracture*, vol. I–VII, Academic Press, New York.
- Main, I., 1992. Earthquake scaling, *Nature*, **357**, 27–28.
- Main, I., 1999. Applicability of time-to-failure analysis to accelerated strain before earthquakes and volcanic eruptions, *Geophys. J. Int.*, **139**, F1–F6.
- Main, I. & Al-Kindy, F., 2002. Entropy, energy and proximity to criticality in global earthquake populations, *Geophys. Res. Lett.*, **29**(7), 1121, doi:10.1029/2000/GL014078.
- Matcharashvili, T., Chelidze, T., Gogiashvili, J. & Tsertsvadze, Z., 2002. Difference in dynamics of distribution and variation of nonlinear correlations in earthquakes temporal, spatial and energetic domains, *Journal of Georgian Geophysical Society*, **7A**, 39–44.
- Meakin, P. & Skjeltorp, A., 1993. Physics of multiparticle systems, *Advances in Physics*, **42**(1), 1–60.
- Miachkin, V., Brace, W., Sobolev, G. & Dietrich, J., 1975. Two Models for earthquake forerunners, *Pure appl. Geophys.*, **113**, 169–181.
- Newman, W.I. & Turcotte, D.L., 2002. A simple model for the earthquake cycle combining self-organized complexity with critical point behavior, *Nonlin. Proces. Geophys.*, **9**, 453–461.

- Nolen-Hoeksema, R.G. & Gordon, R.B., 1987. Optical detection of crack patterns in the opening mode fracture of marble, *Int. J. Rock Mech. Min. Sci.*, **24**, 135–144.
- Petrov, V.A., 1979. On mechanics and kinetics of fracture, *Physics of Solids (Russia)*, **21**, 3681–3686.
- Pike, G. & Seager, C., 1974. Percolation and conductivity, *Phys. Rev.*, **10**, 1421–1435.
- Regel, V., Slutsker, A. & Tomashevsky, E., 1974. *Kinetic nature of strength of solids*. Nauka, Moscow, p. 560 (in Russian).
- Renshaw, C. & Pollard, D., 1994. Numerical simulation of fracture set formation: a fracture mechanics model consistent with experimental observation, *J. geophys. Res.*, **99**, 9359–9372.
- Sahimi, M., 1994. *Applications of Percolation Theory*, Taylor & Francis, London, p. 258.
- Sammis, C. & Sornette, D., 2002. Positive feedback, memory and the predictability of earthquakes, *PNAS*, **99**, (suppl.1) 2501–2508.
- Sawada, Y., Ohta, S., Yamazaki, M. & Honio, H., 1982. Self-similarity and phase-transition-like behaviour of a random growing structure, *Phys. Rev.*, **26**, 3557–3563.
- Scholz, C., 1968. Microfracturing and inelastic deformation of rocks in compression, *J. geophys. Res.*, **73**, 1417–1432.
- Shante, V. & Kirkpatrick, S., 1971. An introduction to percolation theory. *Adv. Phys.*, **20**, 325–357.
- Sobolev, G., 1993. *Fundamentals of Earthquake Prediction*, Nauka, Moscow, p. 313 (in Russian).
- Sornette, D., 2000. *Critical Phenomena in Natural Sciences*, Springer, Berlin-Heidelberg, p. 434.
- Sprott, J. & Rowlands, G., 1995. *Chaos Data Analyzer*, AIP, New York, p. 65.
- Stauffer, D. & Aharony, A., 1992. *Introduction to Percolation Theory*, Taylor & Francis, London, p. 181.
- Tamuž, V. & Kuksenko, V., 1978. *Micromechanics of Destruction of Polymer Materials*. Zinatne, Riga, p. 294 (in Russian).
- Turcotte, D., 2001. Self-organized criticality: does it have anything to do with criticality and is it useful?, *Nonlinear Processes in Geophysics*, **8**, 193–196.
- Voight, B., 1988. A method for prediction of volcanic eruptions, *Nature*, **332**, 125–130.
- Voight, B., 1989. A relation to describe rate-dependent material failure, *Science*, **243**, 200–203.
- Zhurkov, S. & Narzullaev, B., 1953. Time dependence of strength of solids. *Jour. Techn. Physics (Moscow)*, **23**, 1677–1689 (in Russian).
- Zhurkov, S., Kuksenko, V., Petrov, V., Savelyev, V. & Sultanov, U., 1977. On the prognosis of fracture of rocks, *Izvestia Ac. Sci. USSR, Physics of Earth*, No. 6, 1–18, (in Russian).